Electronic Supplementary Information for: Solubility of Cholesterol in Lipid Membranes and Formation of Immiscible Cholesterol Plaques at High Cholesterol Concentrations

Matthew A. Barrett,[1] Songbo Zheng,[1] Laura A. Toppozini,[1] Richard J. Alsop,[1] Hannah Dies,[1] Aili Wang,[1] Nicholas Jago,[1] Michael Moore,[1] and Maikel C. Rheinstädter[1,2,*]

[1] *Department of Physics and Astronomy, McMaster University, Hamilton, ON, Canada*

[2] *Canadian Neutron Beam Centre, National Research Council Canada, Chalk River, ON, Canada*

(Dated: July 24, 2013)

* rheinstadter@mcmaster.ca

I. EFFECT OF HYDRATION ON CHOLESTEROL PLAQUE IMMISCIBILITY

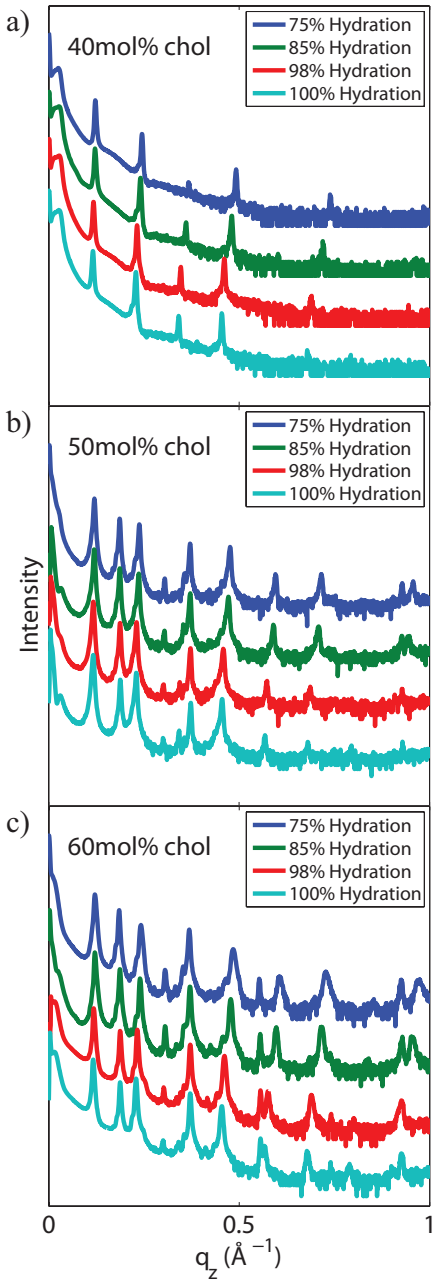

FIG. ESI-1. Out-of-plane scans for DMPC containing a) 40mol%, b) 50mol% and c) 60mol% cholesterol at different levels of hydration.

The structural data presented in this work were measured at T=20° and 50% relative humidity, in a dry state of the membranes. The occurrence of immiscible cholesterol plaques was also checked at higher relative humidities, closer to physiological conditions. Out-

of-plane scans for DMPC containing a) 40mol%, b) 50mol% and c) 60mol% cholesterol are shown in Figure ESI-1. Relative humidities between 75 and 100% were created using saturated salt solutions and the membrane complexes were hydrated from the vapour phase. While the additional signals corresponding to the coexisting immiscible cholesterol phase in the 40mol% sample disappeared with increasing hydration of the membranes, signals corresponding to cholesterol plaques were found to exist at higher cholesterol concentration under full hydration of the membranes. It can, therefore, be speculated that immiscible cholesterol plaques can form under physiological conditions at cholesterol concentrations of more than 40mol%.

II. LAMELLAR SPACINGS FOR ALL MEASURED SAMPLES

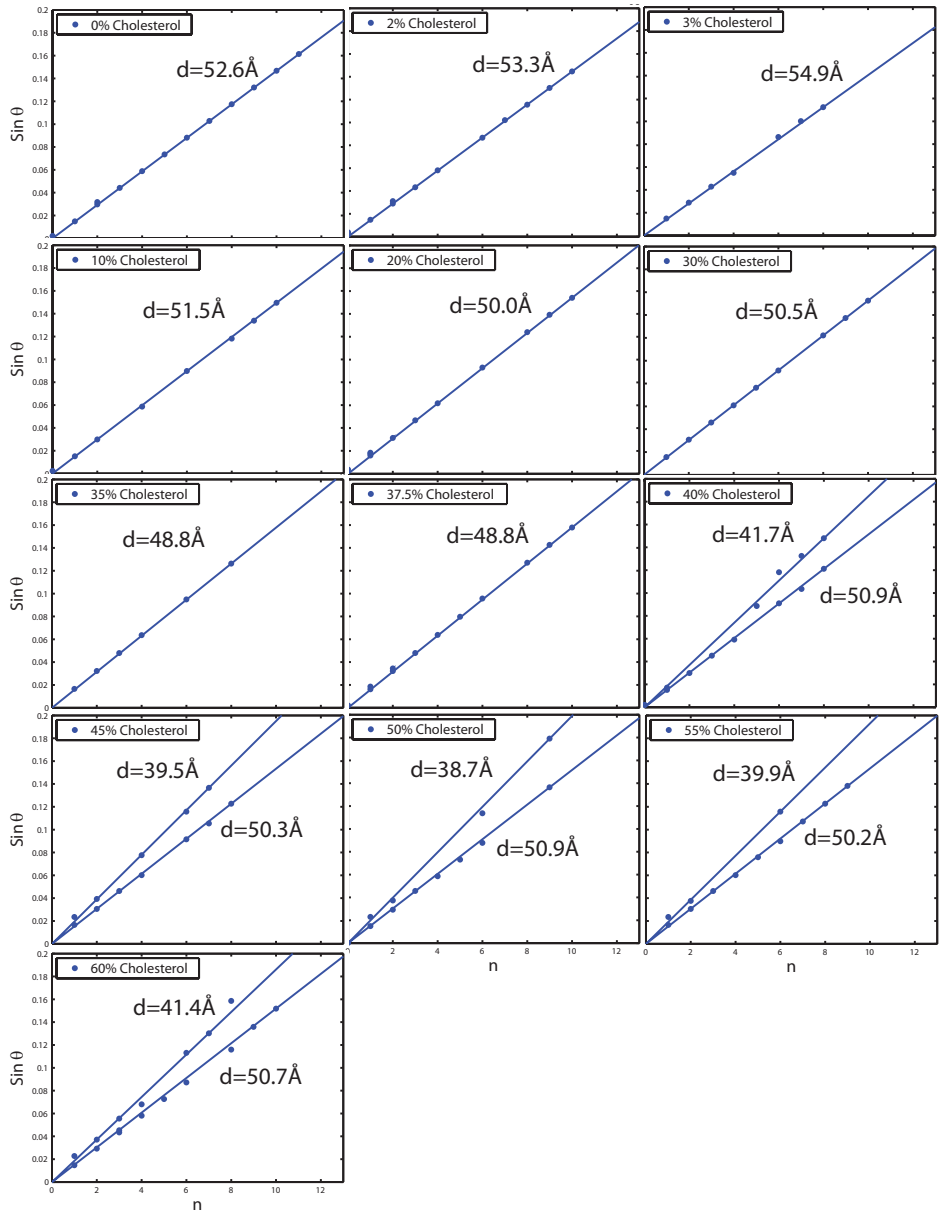

FIG. ESI-2. Order of peaks from the out-of-plane data vs. $\sin(\theta)$, where θ is the Bragg angle. The slope of each line shown is inversely proportional to the distance between membranes in the stack, d_z ($\sin(\theta) = \lambda/(2d_z) \times n$). Values for the different d_z are given in the Figures.

The d_z-spacings for all membrane/cholesterol complexes are shown in Figure ESI-2. Values for the lamellar spacings of lipid and cholesterol bilayer are given in the figures and also in Table I.

III. CRYSTALLOGRAPHIC DETAILS OF THE CHOLESTEROL IN-PLANE STRUCTURES

Miller indices and Bragg angles for the monoclinic and triclinic cholesterol structure at a cholesterol concentration of 55mol% (see Figure 6 e)) are given in Table ESI-1.

monoclinic phase		triclinic phase	
a=10.50 Å, b=8.40 Å, γ=99.7°		$a = b$ =14.2 Å, γ=96.0°	
$[hkl]$	$2\theta\chi$ (°)	$[hkl]$	$2\theta\chi$ (°)
[100]	8.54	[010]	6.27
[010]	10.69	[100]	6.33
$[1\bar{1}0]$	12.52	$[1\bar{1}0]$	8.40
[110]	14.78	[110]	9.39
[200]	17.13	[020]	12.55
$[2\bar{1}0]$	18.63	[200]	12.67
[020]	21.46	$[1\bar{2}0]$	13.42
[210]	21.73	$[2\bar{1}0]$	13.51
$[1\bar{2}0]$	21.74	[120]	14.68
[120]	24.47	[210]	14.76
$[2\bar{2}0]$	25.18	$[2\bar{2}0]$	16.85
[300]	25.82	[220]	18.84
$[3\bar{1}0]$	26.26	[030]	18.78
[310]	29.68	[300]	19.06

TABLE ESI-1. Miller indices, $[hkl]$, and in-plane Bragg angles, $2\theta\chi$, for monoclinic and triclinic bilayer cholesterol phases at a cholesterol concentration of 55mol% (see Figure 6 e)).